

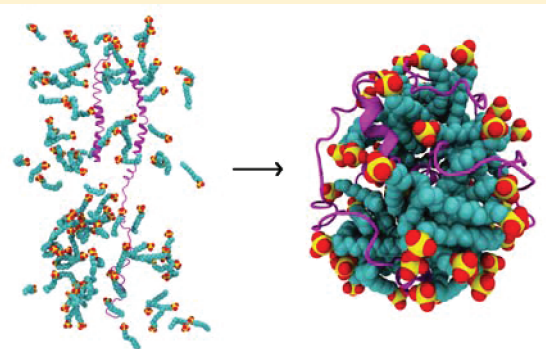
# Characterization of a Disordered Protein during Micellation: Interactions of $\alpha$ -Synuclein with Sodium Dodecyl Sulfate

Jianhui Tian,<sup>†</sup> Anurag Sethi,<sup>†</sup> Divina Anunciado,<sup>‡</sup> Dung M. Vu,<sup>‡</sup> and S. Gnanakaran\*,<sup>†</sup>

<sup>†</sup>Theoretical Biology and Biophysics Group, and <sup>‡</sup>Physical Chemistry and Applied Spectroscopy, Los Alamos National Laboratory, Los Alamos, New Mexico 87545, United States

 Supporting Information

**ABSTRACT:** To better understand the interaction of  $\alpha$ -synuclein ( $\alpha$ Syn) with lipid membranes, we carried out self-assembly molecular dynamics simulations of  $\alpha$ Syn with monomeric and micellar sodium dodecyl sulfate (SDS), a widely used membrane mimic. We find that both electrostatic and hydrophobic forces contribute to the interactions of  $\alpha$ Syn with SDS. In the presence of  $\alpha$ Syn, our simulations suggest that SDS aggregates along the protein chain and forms small-size micelles at very early times. Aggregation is followed by formation of a collapsed protein–SDS micelle complex, which is consistent with experimental results. Finally, interaction of  $\alpha$ Syn with preformed micelles induces alterations in the shape of the micelle, and the N-terminal helix (residues 3 through 37) tends to associate with micelles. Overall, our simulations provide an atomistic description of the early time scale  $\alpha$ Syn–SDS interaction during the self-assembly of SDS into micelles.



## INTRODUCTION

$\alpha$ -Synuclein ( $\alpha$ Syn) is an intrinsically disordered protein that is abundantly expressed in the brain.<sup>1</sup> It is localized at the nerve termini in close proximity to synaptic vesicles.<sup>2,3</sup> Its native function is thought to involve vesicle maintenance and recycling, modulation of neural plasticity, endoplasmic reticulum-Golgi trafficking, and dopamine reuptake.<sup>1,4–8</sup> Numerous studies have implicated the involvement of  $\alpha$ Syn in Parkinson's disease (PD), as it has been found to be the major protein component of Lewy bodies and Lewy neurites, which are the two major hallmarks of the disease.<sup>9,10</sup> However, it is still not clear how  $\alpha$ Syn executes its function, and what are its toxic forms and key conformations for fibril formation.

$\alpha$ Syn is a relatively small protein (140 residues) with low sequence complexity, low hydrophobicity, and a high net charge. It includes seven imperfect 11-residue repeats in its N-terminus, six of which contain a highly conserved motif, KTK(E/Q)GV, which forms  $\alpha$ -helices in association with membranes.<sup>11</sup> The N-terminus (residues 1–60) is observed to trigger binding of the protein with membrane and nucleates  $\alpha$ -helix formation.<sup>12,13</sup> The middle region (residues 61–95) is called the NAC (non- $\text{A}\beta$  component of Alzheimer's disease amyloid) region and is particularly hydrophobic, with only three charged residues at Glu61, Lys80, and Glu83. The C-terminus (residues 96–140) is highly acidic and proline-rich and contains three highly conserved tyrosine residues. It is believed to play an important role in the regulation of  $\alpha$ Syn aggregation and fibrillation.<sup>14–19</sup>

In solution, monomeric  $\alpha$ Syn has no well-defined structure but appears to be more compact than a random-coil

conformation.<sup>20,21</sup> Recently, Bartels et al. found that native  $\alpha$ Syn exists in cells as a helically folded tetramer.<sup>22</sup> The functionality of  $\alpha$ Syn is expected to involve its interaction with membrane. When interacting with lipid vesicles or membranes,  $\alpha$ Syn displays two different conformations, a helix-turn-helix structure or an extended helical structure, depending on the curvature of the binding surface.<sup>23–25</sup> In the helix-turn-helix conformation, the first helix occurs between residues 3 and 37 (helixN) and the second helix occurs between residues 45 and 92 (helixC). Lipid vesicle compositions have also been shown to affect the binding strength of  $\alpha$ Syn.<sup>26</sup> Both electrostatic and hydrophobic interactions are important in the association of  $\alpha$ Syn with lipid bilayers, and this association can lead to changes in the physical properties of bilayers.<sup>27</sup>

As a lipid membrane mimic, sodium dodecyl sulfate (SDS) has been widely used to study the role of lipid binding in modulating the conformational changes of  $\alpha$ Syn as well as its aggregation process.<sup>28–36</sup> Ferreon et al. observed a conformational interconversion between unfolded, helix-turn-helix and extended helices from isothermal protein–SDS titration experiments.<sup>28</sup> The fibrillation pathways of  $\alpha$ Syn have been shown to differ in the presence and absence of SDS.<sup>32</sup> In addition, fibrillation occurs only at low concentrations of SDS surfactant.<sup>37</sup>

Despite extensive experimental work on  $\alpha$ Syn, its interaction with lipid bilayers/micelles and its aggregation effects are still

Received: October 27, 2011

Revised: February 28, 2012

Published: March 22, 2012



not well understood at the molecular level. A limited number of simulation studies have been performed to complement the experimental studies. Wu et al. compared  $\alpha$ Syn conformations in neutral and low pH conditions using replica exchange molecular dynamics and found that C-terminal compaction is key to the rapid aggregation at low pH.<sup>15</sup> Mihajlovic et al. studied the structure and energetics of the N-terminus of  $\alpha$ Syn bound to membrane using implicit membrane models.<sup>38</sup> They found that the truncated protein (1–9Saa) shows a bent 11/3 helix conformation on the mixed membrane. The preference for 11/3 helix is associated with collective motion and a favorable solvation energy. Perlmutter et al. compared the dynamics of the three PD related mutations with wild-type  $\alpha$ Syn in micelle and in bilayer-bound forms.<sup>39</sup> They demonstrated that  $\alpha$ Syn and its variants are less dynamic in the bilayer than in the micelle. Despite these studies, the mechanism of how  $\alpha$ Syn interacts with micelles/membranes and its associated protein conformational changes are poorly understood.

In this study, we conduct comprehensive molecular dynamics simulations of  $\alpha$ Syn with self-assembling and self-assembled SDS micelle systems. Despite the fact that SDS has long been used as a protein denaturant,<sup>40</sup> the exact nature of the interactions between SDS and protein is still being extensively studied.<sup>41–43</sup> A “necklace-model” has been proposed for the SDS micelle–protein interaction beyond SDS critical micellar concentration.<sup>44</sup> There are two versions for the model: (1) the aggregation model, where the hydrophobic patches along the protein chain acts as an aggregation site for micelle growth, and (2) the wrap model, where proteins wrap around the micelles during the interacting process. However, the mechanism of how SDS forms micelles in the presence of a protein remains to be answered. Here, we aim to dissect the driving force between  $\alpha$ Syn and SDS interactions leading to conformational changes of  $\alpha$ Syn during SDS micellation, and to characterize the influence of  $\alpha$ Syn on SDS micellation.

## METHODS

**$\alpha$ Syn Interaction with SDS Monomers.** We studied quaternary systems that are composed of  $\alpha$ Syn, SDS, NaCl, and water. Two conformations of  $\alpha$ Syn were explored: the helix-turn-helix conformation as deduced from NMR structure (PDB ID 1XQ8)<sup>30</sup> and an extended random-coil-like conformation generated by simulating the helix-turn-helix conformation at 600 K for 5 ns. This extended conformation had a backbone root-mean-square deviation (rmsd) of 2.28 nm compared to the helix-turn-helix conformation.

Georgieva et al.<sup>45</sup> found that the ratio of detergent to protein, in addition to absolute concentration of detergent, can influence  $\alpha$ Syn conformation. Therefore, we carried out simulations with two different ratios, 100:1 and 200:1 of SDS to folded/unfolded  $\alpha$ Syn, to explore how this ratio could affect the distribution of conformations. These ratios were above the 70:1 ratio required for proper solvation as found by Ulmer et al.<sup>30</sup> This choice ensured that we had a sufficient number of SDS molecules necessary to interact with  $\alpha$ Syn.

Finally,  $\text{Na}^+$  and  $\text{Cl}^-$  ions were added in the system to act as counterions for charged amino acid side chains and to make a physiological ionic concentration of 0.15 M. Table 1 shows the different simulations conducted. All systems were simulated twice using different seeds for initial velocity to verify the results. Initially,  $\alpha$ Syn is placed in the center of the unit box and SDS is randomly distributed without overlapping with  $\alpha$ Syn.

**Table 1. Different Simulations Considered in This Study<sup>a</sup>**

system	SDS no.	water no.	SDS concn (mM)	init protein conformation	time (ns)
200Folded	200	46602	238	helix-turn-helix	200
200Unfold	200	46623	238	unfold extended	200
100Folded	100	48331	115	helix-turn-helix	200
MicelleFolded	270	54105	277	helix-turn-helix	200
MicelleUnfold	270	54103	277	unfold extended	200
200SDS <sup>b</sup>	200	47385	234	N/A	200

<sup>a</sup>The number of SDS molecules and the initial configurations of  $\alpha$ Syn are varied. <sup>b</sup> $\alpha$ Syn is not present in the system simulated.

The systems were first energy minimized and then gradually heated to 323 K during the first 300 ps. During the minimization and heating up process, the position of  $\alpha$ Syn was restrained with a harmonic potential to avoid unwanted conformational change. The production runs were conducted at constant pressure (1 atm) and constant temperature (323 K). At this temperature the SDS forms micelles successfully<sup>46,47</sup> and the force field we use shows a weak temperature dependence for protein conformations.<sup>48,49</sup>

GROMACS-4.5.1 package was used for all the simulations.<sup>50</sup> OPLS-AA force field was used for  $\alpha$ Syn, as Sgourakis et al.<sup>51</sup> found that OPLS-AA force field gave good agreement to experimental results by studying disordered protein A $\beta$  40/42. A GROMOS based force field that has been used successfully by Sammalorpi et al.<sup>46,47</sup> to study micelle formation was employed for SDS. Explicit water molecules were modeled using the simple-point-charge (SPC) water model that was included in the GROMACS package. During NPT production run, Nose–Hoover thermostat was used for temperature control with a 1.0 ps coupling constant,<sup>52,53</sup> and Parrinello–Rahman extended-ensemble coupling was used for pressure control with a coupling constant of 0.5 ps.<sup>54</sup> Electrostatics were treated using the particle mesh Ewald method<sup>55</sup> with a 1.0 nm real space cutoff. The van der Waals interactions were treated using a 1.0 nm cutoff and energy and pressure dispersion correction is employed. All bond interactions involving hydrogen atoms were constrained using SETTLE<sup>56</sup> and LINCS<sup>57</sup> to allow for a 2 fs integration time step. All the simulations have been run for 200 ns with frames saved every 4 ps.

**$\alpha$ Syn Interaction with Preformed SDS Micelles.** In addition to its interaction with monomeric SDS molecules, we also considered the interaction of  $\alpha$ Syn with preformed SDS micelles. Interactions of both folded (helix-turn-helix) and unfolded conformations of  $\alpha$ Syn with four preformed micelles were considered. Two of the four micelles were composed of 86 SDS and the other two micelles were composed of 49 SDS. These numbers are consistent with the number of SDS per micelle in Ulmer et al.’s experiments.<sup>30</sup> The simulation conditions and procedure used for this study were identical to  $\alpha$ Syn interaction with SDS monomers. The system was simulated for 200 ns to explore the interaction between free  $\alpha$ Syn and SDS micelles.

## RESULTS

**Nonspecific Interaction between  $\alpha$ Syn and SDS Monomers.** During the simulations of the self-assembly of SDS micelles, monomeric SDS freely diffuses and interacts with the independently diffusing  $\alpha$ Syn molecule. It binds  $\alpha$ Syn and forms small aggregates around the whole protein. The

interaction between  $\alpha$ Syn and monomeric SDS is tracked by calculating the number of sulfate headgroup (OS, S, and O) atoms and alkyl chain carbon atoms within 0.35 nm of protein atoms as a function of time for all simulations. Alkyl chain carbon atoms of SDS molecules preferentially interact with the  $\alpha$ Syn. Figure 1 shows this profile for the 200Folded system.

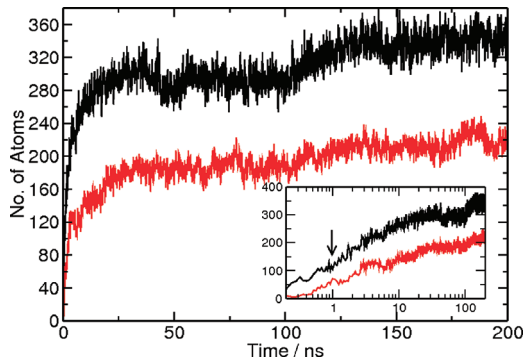


**Figure 1.** Number of SDS headgroup atoms (OS, S, and O) (red line) and alkyl tail atoms (black line) within 0.35 nm of the protein as a function of time for  $\alpha$ Syn started from helix-turn-helix conformation in the 200Folded system. Inset captures the early events by considering the same plot with time on a logarithmic scale.

Only the interactions involving the first shell of SDS with protein is tabulated, eliminating any necessity for the normalization of the number of alkyl chain carbon atoms, sulfate head groups, and oxygen atoms.

This observed preference indicates that the interaction between  $\alpha$ Syn and SDS is not solely driven by the electrostatic interactions between the positively charged side chain of protein and the negatively charged sulfate head groups, but there is also a significant contribution from the hydrophobic interaction between SDS tails and the apolar amino acids. Our observation clearly confirms previous experimental results showing that the hydrophobic interaction plays an important role in SDS–protein interactions.<sup>41,58</sup> On the basis of multiple simulations, we do not observe any specific residues of  $\alpha$ Syn that make preferential contacts with SDS molecules. We interpret this to mean that monomeric SDS interaction with the protein is nonspecific.

**SDS Micellation around  $\alpha$ Syn.** During micellation, we observe that SDS interacts with  $\alpha$ Syn and forms a stable micelle–protein collapsed complex. As shown in Figure 2, the micelle formation and the interaction with the  $\alpha$ Syn occur simultaneously. On the basis of our simulations, we propose a three-stage process for initial micelle formation. First, monomeric SDS interacts nonspecifically with  $\alpha$ Syn and forms small aggregates along the protein chain. Next, the

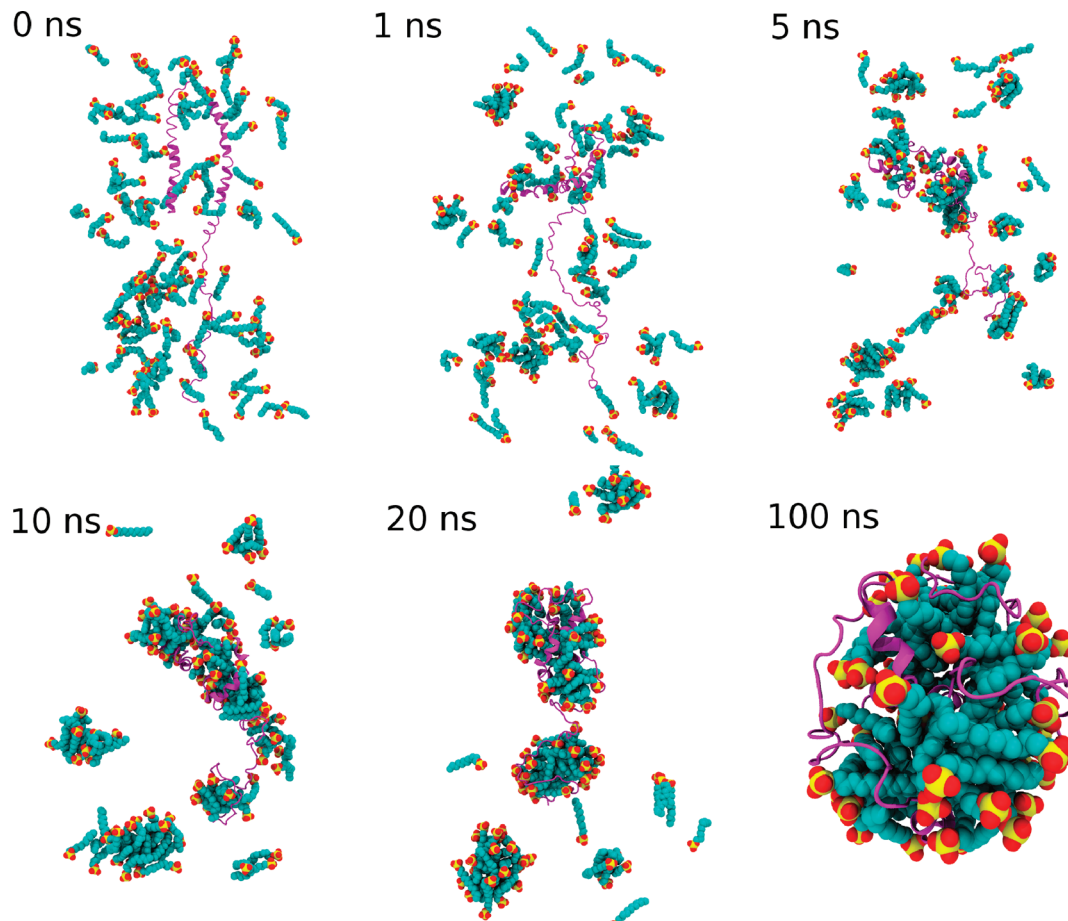


**Figure 2.** Snapshots of SDS micellation at 0, 1, 5, 10, 20, and 100 ns from the 100Folded system. Only the  $\alpha$ Syn and SDS in the final complex are shown in the snapshot for clarity. The  $\alpha$ Syn is in magenta cartoon presentation. The SDS molecules are in space-filling representation, while the head groups are in red and yellow and the alkyl carbon tails are in cyan. SDS monomers, which are not part of the final complex, are not shown for clarity. The snapshots are made in VMD.<sup>59</sup>

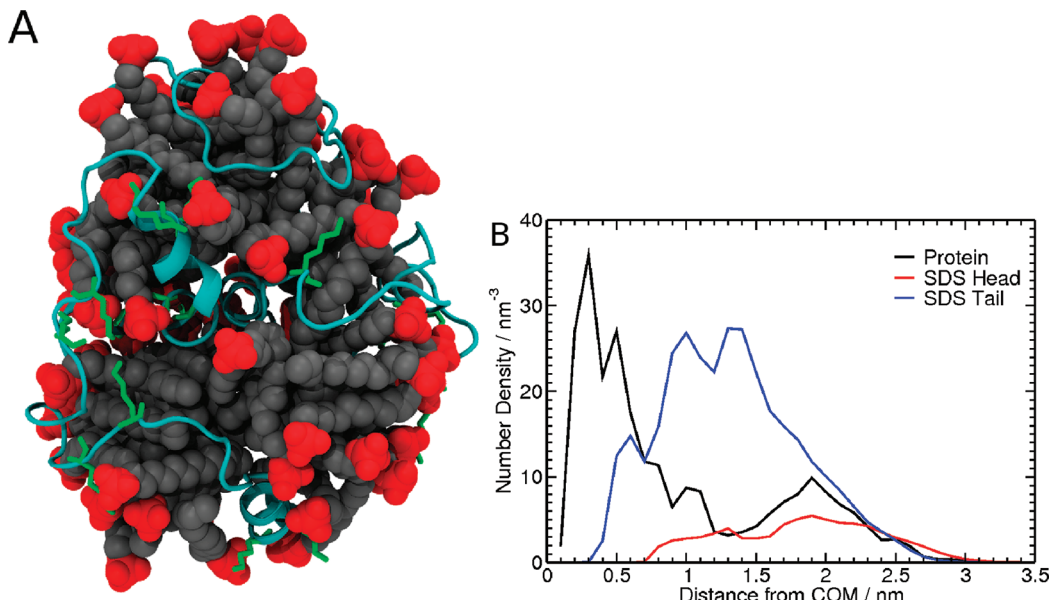


**Figure 3.** Conformation of an  $\alpha$ Syn–SDS complex at the end of the 100Folded system. The image shows the structure at the end of the 100Folded simulation. (A) The complex with  $\alpha$ Syn in cyan cartoon presentation, and SDS in space-filling representation. Headgroup atoms of SDS are in red, lysine residues of  $\alpha$ Syn are in green sticks. (B) The density profile for different components from the center of mass of the complex along the radial direction.

small aggregates grow by micelle fusion while the collapse of  $\alpha$ Syn at the same time appears to promote the fusion process. Finally, it forms a collapsed  $\alpha$ Syn–SDS micelle complex. These different stages of micelle formation appear to be very similar to the process of reverse micelle self-assembly process as studied by Tian et al.<sup>60,61</sup> These findings clearly support an aggregation model for the  $\alpha$ Syn–SDS interaction. Bhuyan et al. observed a similar behavior in their experimental work<sup>41</sup> on cytochrome *c* protein. Despite the inherent structural dissimilarity between intrinsically disordered proteins and structured proteins, it appears that the interactions of these two types of proteins with SDS are similar.

**Conformation of  $\alpha$ Syn–SDS Complex.** Simulations of all three  $\alpha$ Syn–SDS monomer systems (200Folded, 200Unfold, and 100Folded) lead to a collapsed protein–SDS micelle complex. The structure of the final collapsed  $\alpha$ Syn–SDS complex from the 100Folded system resulted in a total of 64 SDS molecules in the complex with a radius of gyration of 1.9 nm (Figure 3A). Residues 68 to 80 from the NAC region are buried in the center of the micelle by SDS molecules. Residues 101 to 140 of the C-terminus wrap around the micelle and lay on the surface with one side in contact with SDS micelle and the other side with waters. The lysine side chains are highly coordinated to the SDS head groups while the glutamic acid side chains are solvated by water molecules (Figure S1 in the Supporting Information). In Figure 3B, the density profiles for the  $\alpha$ Syn and SDS are shown in relation to the center of mass of the complex. Protein atoms have a wide distribution in the complex, which covers from the center of mass to the surface, and the atoms close to the core result in an overall high density in the plot. This also confirms the aggregation model for the protein–SDS interactions because the protein density can only be expected to be on the surface of the complex if it is the wrap model. In the case of SDS, even with the interaction of bound  $\alpha$ Syn, the complex shows a density profile similar to a typical micelle.

**Conformational Variability of  $\alpha$ Syn during Micellation.** Next, we characterize the global changes in  $\alpha$ Syn conformation during the micellation by considering radius of gyration ( $R_g$ ) and end-to-end ( $N2N$ ) distance. Figure 4 and

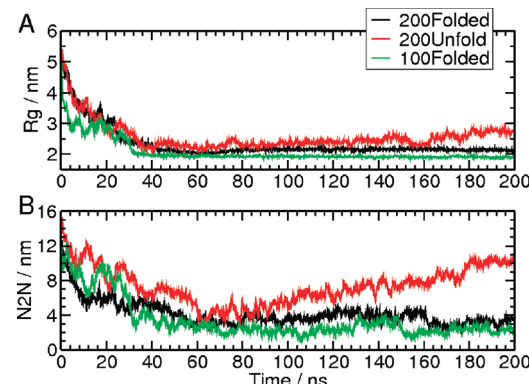


**Figure 4.** Global conformational changes of  $\alpha$ Syn in the 200Folded, 200Unfolded, and 100Folded systems as a function of time. The first plot shows the radius of gyration, the second plot shows the end-to-end ( $N2N$ ) distance.

Figure S2 (in the Supporting Information) show  $R_g$  and  $N2N$  for the three systems: 200Folded, 200Unfold, and 100Folded. In all three simulations,  $\alpha$ Syn initially collapses to conformations with  $R_g$  about 2.2 nm within 40 ns. Then, it remained constant in 200Folded and 100Folded systems where simulations were started from the helix-turn-helix conformation with 200 and 100 SDS molecules, respectively. It expanded slightly to 2.8 nm in 200Unfold system where the simulations were started from the unfolded extended conformation with 200 SDS molecules.

**Changes in Secondary Structural Content of  $\alpha$ Syn during Micellation.** In the 200Folded and 100Folded systems,  $\alpha$ Syn in helix-turn-helix conformation unfolds within a short time. About two-thirds of the helical content of the

folded conformation is lost within first 10 ns during the micellation process. However, ~10 residues remain helical during the entire simulation (Figure 5A, and Figure S3 in the

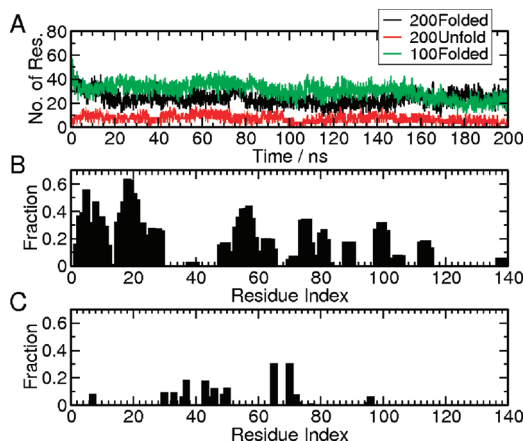


**Figure 5.** Secondary structure propensity for each of the residues in the  $\alpha$ Syn which is calculated from the average of the three  $\alpha$ Syn–SDS monomer interaction systems.

Supporting Information). They interact strongly with SDS aggregates or micelles. These observations from simulations agree with the study of Gambin et al.<sup>34</sup> which reported on a ligand-bound collapsed complex after the initial mixing of  $\alpha$ Syn with SDS. Also, an intermediate helix-turn-helix  $\alpha$ Syn structure after 1.2 ms of the mixing reaction was observed in that study. Because of the current computational limitations, we cannot explore the folding of the protein after the formation of a protein–SDS micelle complex.

Next, we consider nonrigorous quantification of the secondary structure propensity at residue level by calculating the average helix and  $\beta$ -sheet percentage of the three systems (Figure 5B,C). Residues 1 to 30 have a high helical structure propensity; residues 31 to 45 and 106 to 140 have no helical propensity, while residues 46 to 106 display intermediate helical propensity, with some interruptions. Residues 31 to 100 show a  $\beta$ -sheet structure propensity. Three interruptions in helical propensity are observed in Figure 5 for the N-terminus: residues 30 to 47, 66 to 69, and 83 to 87, all of which agree very well with the experimentally measured regions with interruptions in helicity as shown by Bigaglia et al.<sup>33</sup> and Bussell et

al.<sup>11</sup> We note that the starting structure from a helix-turn-helix or extended unfolded conformation will affect the absolute value of the secondary structure fraction, but the preference for residues 1 to 30 to form a helix and for 31 to 100 to form a  $\beta$ -sheet will not change.

**$\alpha$ Syn Interaction with Preformed SDS Micelles.** Next we considered the interaction of  $\alpha$ Syn with SDS micelles rather than with SDS monomeric molecules. Preformed micelle systems contained 270 SDS molecules in four micelles and one  $\alpha$ Syn in extended random-coil or helix-turn-helix conformation. In both preformed micelle systems,  $\alpha$ Syn bound to multiple micelles and collapsed from the extended random-coil or helix-turn-helix structure to a more compact structure during the simulation. The N-terminal and C-terminal domains both interact with micelles. In the MicelleFolded simulations, we observe that the helical contents of helixN and helixC decrease rapidly even before they bind and interact with micelles. The collapse of  $\alpha$ Syn brings micelles together and may promote the fusion of micelles.

The solvent-accessible surface area (SASA) for helixN and helixC are shown in Figure 6A and Figure S5 in the Supporting Information for MicelleFolded simulations. For reference, SASA values for helixN and helixC in bulk water are  $0.95 \text{ nm}^2/\text{residue}$  and  $0.81 \text{ nm}^2/\text{residue}$ , respectively. When interacting with SDS micelles, the SASA for helixN decreases monotonically and reaches a plateau after 100 ns simulation time with a final magnitude of  $0.38 \pm 0.02 \text{ nm}^2/\text{residue}$ . The solvent exposure is 40% of the magnitude in bulk water. On the other hand, SASA for helixC also decreases monotonically as a function of simulation time, however, the magnitude of the SASA displays much larger fluctuations after the initial decrease. The average SASA for the last 10 ns simulation is  $0.46 \pm 0.02 \text{ nm}^2/\text{residue}$ , which is about 57% of the magnitude in bulk water. Figure 6A (inset) and Figure S5 show the average area per residue for helixN and helixC in contact with SDS molecules. We notice that both curves increased during the first 100 ns. Then the contacts are saturated with helixN having a larger contact area. These findings suggest that the helixN interacts more with the micelle hydrophobic interior, whereas helixC lies on the micelle surface with more exposure to water. This is consistent with the HelixN preserving residual helical structures during the interaction with micelles (Figure S4 in the Supporting Information). This higher stability of helixN over helixC is consistent with experimental results, which show that

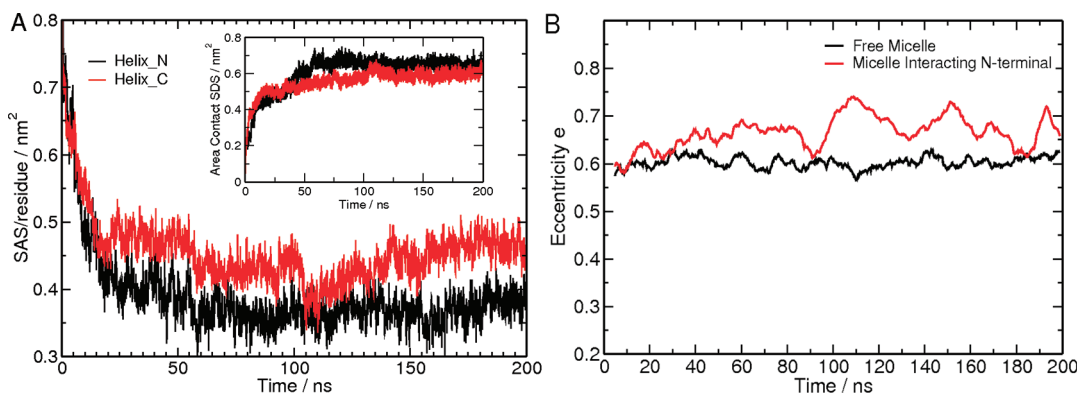


**Figure 6.** (A) Solvent-accessible surface area (SASA) per residue for helixN and helixC as a function of time for the whole simulation time. Inset shows the surface area of protein per residue in contact with SDS molecules as a function of time. (B) Eccentricity of micelles as a function of time. Perfect sphere has an eccentricity of 0 and a rod has an eccentricity of 1.

the N-terminus of  $\alpha$ Syn triggers membrane binding and helix folding.<sup>12</sup> In addition, helixN is also known to bind to membranes more strongly than helixC.<sup>62</sup>

Furthermore, the interaction of  $\alpha$ Syn with SDS micelle induces alterations in micelle shapes. The eccentricity for two micelles as a function of time is shown in Figure 6B. Here, the eccentricity measures the degree of deviation from a sphere of an ellipsoidal shape with 0 for a perfect sphere and 1 for a rod. The eccentricity for the free micelle is constant with small fluctuations; while the micelle interacting with the N-terminal of  $\alpha$ Syn shows deviations in shape. We observe significant flattening of the face of the micelles interacting with  $\alpha$ Syn in the simulation. This could explain the discrepancy in the curvature of a micelle formed by ~70 SDS molecules and that of a helix-turn-helix conformation of  $\alpha$ Syn.<sup>30</sup>

#### Micellation of SDS Monomers with and without $\alpha$ Syn.

Finally, we considered a control simulation of 200 SDS molecules (200SDS system) in the absence of  $\alpha$ Syn. This simulation was identical to the previous simulation of 200Unfold system, except that the protein was replaced by water molecules and the total charge of the system was balanced by adding/deleting sodium chloride ions. We note that the total volume of the system remained constant with the replacement of protein by water. The number of micelles as a function of time for the systems with and without  $\alpha$ Syn is plotted in Figure 7, where we used the same definition for

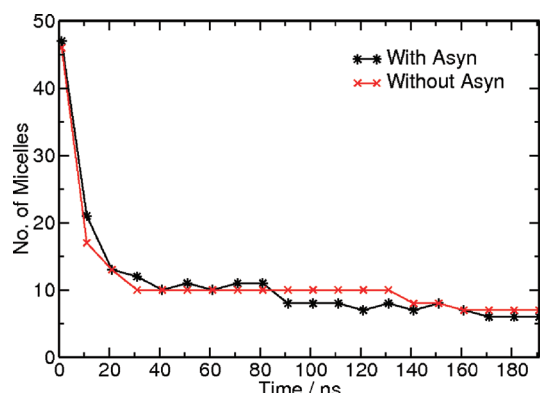


Figure 7. Number of micelles as a function of simulation time for the system with and without  $\alpha$ Syn.

Table 2. Number of SDS Molecules in Each of the Micelles

micelle ID	1	2	3	4	5	6	7
with $\alpha$ Syn	15	22	25	44	44	50	
without $\alpha$ Syn	15	23	24	33	34	35	36

micelles as used in Sammalorpi et al.'s work.<sup>46</sup> The two plots are similar, which indicates that the presence of  $\alpha$ Syn did not change the overall micellation process. However, there are fewer micelles at the end of the simulation, and the size of the micelles is less homogeneous in the system with  $\alpha$ Syn than in the simulation without  $\alpha$ Syn (Table 2). Therefore, the protein can affect the nature of the micelles. These findings were further verified by performing another set of comparison simulations with and without extended  $\alpha$ Syn in the 200SDS self-assembly system.

#### DISCUSSION

$\alpha$ Syn is disordered in bulk solvent but is more compact compared to the radius of gyration expected for a self-avoiding polypeptide chain of the same size (4.1 nm).<sup>21</sup> The deposition of  $\alpha$ Syn fibrils is characterized by rich  $\beta$ -sheet structure of residues 31 to 100.<sup>63</sup> It adopts various helical conformations when interacting with SDS micelles or lipid membranes. In this study, we have characterized the early interactions of  $\alpha$ Syn with SDS to gain a better understanding of the role that lipid plays in the conformational changes of  $\alpha$ Syn.

Two conformations, a helix-turn-helix conformation and an extended helix conformation, have been consistently observed for  $\alpha$ Syn in lipophilic environment. However, the stability and the flux of the helical conformations of  $\alpha$ Syn as it interacts with lipid membranes or micelles have been shown to be complex. Bodner et al. reported multiple tight phospholipid binding modes and showed that the C-terminal region interacts with lipid at high lipid concentration.<sup>64,65</sup> They also found that helix formation is required for the association of  $\alpha$ Syn to lipid membrane during which the transient helix is stabilized by interaction with the membrane. This implies a selective mechanism for  $\alpha$ Syn interaction with membrane. Our study here shows that  $\alpha$ Syn helix conformation is not stable without interaction with SDS micelle. Helix unfolds in a time scale of 10 ns, while the formation of SDS micelle occurs in the time scale of 100s of nanoseconds, which is inconsistent with the selective mechanism.

During micellation, SDS interacts with  $\alpha$ Syn nonspecifically and aggregates around the chain of the protein. This can explain why no clear critical micellar concentration is identified with  $\alpha$ Syn in the study by Ahmad et al.<sup>37</sup> Regardless of whether we consider a folded or an unfolded  $\alpha$ Syn as an initial configuration,  $\alpha$ Syn unfolds before forming a collapsed complex which is consistent with Gambin et al.'s<sup>34</sup> experimental results. The collapsed complex should be followed by the formation of secondary structure of  $\alpha$ Syn in the microsecond time scale, which is beyond the scope of our current simulation limits.

By comparing two sets of simulations with different numbers of SDS molecules, we explored the influence of SDS to protein ratio during the self-assembly process. We find a slight increase in micelle formation in the system where a single  $\alpha$ Syn is considered with 200 SDS molecules compared to a system with 100 SDS molecules. This is the result of increased contacts between  $\alpha$ Syn and SDS micelles at the higher SDS to protein ratio, and one could expect that the SDS ratio may further influence the formation of protein secondary structure at even higher ratios. Past studies have implied that the electrostatic interactions between anionic SDS headgroup and cationic amino acid side chains as critical during micellation. Our calculations indicate that both electrostatic and hydrophobic interactions contribute to  $\alpha$ Syn's association with SDS micelles.

Finally,  $\alpha$ Syn can potentially affect the lipid membrane as changes to the membrane properties are observed in association with the protein.<sup>27</sup> Our comparative study of SDS micellation with and without  $\alpha$ Syn showed that, while the overall micellation process is not significantly affected, the size of micelles with  $\alpha$ Syn in the system is more heterogeneous than without  $\alpha$ Syn. According to simulations of  $\alpha$ Syn with preformed micelles, both N-terminal and C-terminal regions interact with micelles with N-terminal helix exhibiting a slight preference for association. Furthermore,  $\alpha$ Syn induces slight alterations in micelle shapes that possibly explain the

discrepancy in the curvature of a micelle formed by ~70 SDS molecules and that of a helix-turn-helix conformation of  $\alpha$ Syn.<sup>30</sup>

## CONCLUSIONS

We performed molecular dynamics simulations to characterize the conformational variability of  $\alpha$ -synuclein ( $\alpha$ Syn) during self-assembly of sodium dodecyl sulfate (SDS) molecules into micelles. The interactions of  $\alpha$ Syn with SDS monomers and SDS micelles were explored during the micellation process. Both electrostatic and hydrophobic forces contribute to the interaction between the  $\alpha$ Syn and SDS. The  $\alpha$ Syn–SDS interaction can be best described by the aggregation version of the necklace-bead model. The mixing of  $\alpha$ Syn with SDS initially forms a collapsed complex that is followed by the folding of the protein in a microsecond time scale. When interacting with SDS,  $\alpha$ Syn exhibits secondary structural content with residues 1 to 30 having a high helix propensity and residues 31 to 100 having a  $\beta$ -sheet propensity. When interacting with preformed SDS micelle, the N-terminal helix associates more with micelles. Overall, our simulation results agree well with many of the available experimental results.<sup>11,12,33,34,37,41,58,62</sup> Importantly, our simulations provide valuable microscopic insight into the nature of the  $\alpha$ Syn–SDS interactions, which will be useful for future experimental design of intrinsic disordered protein–membrane systems.

## ASSOCIATED CONTENT

### Supporting Information

Figures S1–S5 show interactions of charged residues from  $\alpha$ Syn with SDS and water and confirmation of results from additional simulations. S1: radial distribution function of lysine and glutamic acid side chain to SDS head group and water molecules; S2: global conformational changes of  $\alpha$ Syn in the second sets of simulations of 200Folded, 200Unfolded, and 100Folded systems as a function of time; S3: number of residues in the helix structure as a function of time for the second sets of simulations of 200Folded, 200Unfold, and 100Folded systems; S4: evolution of the secondary structure for each of the residues as a function of time for the two preformed micelle simulations; S5: solvent-accessible surface area (SASA) per residue for helixN and helixC as a function of time for the second preformed micelle simulation. This material is available free of charge via the Internet at <http://pubs.acs.org>.

## AUTHOR INFORMATION

### Corresponding Author

\*E-mail: gnana@lanl.gov.

### Notes

The authors declare no competing financial interest.

## ACKNOWLEDGMENTS

This work was supported by LANL/LDRD grant X9C4, NIH grant R37-GM035556, and the LANL Institutional Computing for the supercomputer time. A.S. was supported by a postdoctoral fellowship from the Center for Nonlinear Studies. We thank Byron Goldstein for his suggestions and commitments for writing the manuscript and Jennifer Macke for editing the manuscript.

## REFERENCES

- (1) George, J. M.; Jin, H.; Woods, W. S.; Clayton, D. F. *Neuron* **1995**, 15, 361.
- (2) Jensen, P. H.; Nielsen, M. S.; Jakes, R.; Dotti, G.; Goedert, M. J. *Biol. Chem.* **1998**, 273, 26292.
- (3) Iwai, A.; Maslia, E.; Yoshimoto, M.; Ge, N. F.; Flanagan, L.; Desilva, H. A. R.; Kittel, A.; Saitoh, T. *Neuron* **1995**, 14, 467.
- (4) Sidhu, A.; Wersinger, C.; Vernier, P. *FEBS Lett.* **2004**, 565, 1.
- (5) Sudhof, T. C.; Chandra, S.; Fornai, F.; Kwon, H. B.; Yazdani, U.; Atasoy, D.; Liu, X. R.; Hammer, R. E.; Battaglia, G.; German, D. C.; Castillo, P. E. *Proc. Natl. Acad. Sci. U.S.A.* **2004**, 101, 14966.
- (6) Rosenthal, A.; Abeliovich, A.; Schmitz, Y.; Farinas, I.; Choi-Lundberg, D.; Ho, W. H.; Castillo, P. E.; Shinsky, N.; Verdugo, J. M. G.; Armanini, M.; Ryan, A.; Hynes, M.; Phillips, H.; Sulzer, D. *Neuron* **2000**, 25, 239.
- (7) Murphy, D. D.; Rueter, S. M.; Trojanowski, J. Q.; Lee, V. M. Y. *J. Neurosci.* **2000**, 20, 3214.
- (8) Cooper, A. A.; Gitler, A. D.; Cashikar, A.; Haynes, C. M.; Hill, K. J.; Bhullar, B.; Liu, K. N.; Xu, K. X.; Strathearn, K. E.; Liu, F.; Cao, S. S.; Caldwell, K. A.; Caldwell, G. A.; Marsischky, G.; Kolodner, R. D.; LaBaer, J.; Rochet, J. C.; Bonini, N. M.; Lindquist, S. *Science* **2006**, 313, 324.
- (9) Baba, M.; Nakajo, S.; Tu, P. H.; Tomita, T.; Nakaya, K.; Lee, V. M. Y.; Trojanowski, J. Q.; Iwatsubo, T. *Am. J. Pathol.* **1998**, 152, 879.
- (10) Spillantini, M. G.; Schmidt, M. L.; Lee, V. M. Y.; Trojanowski, J. Q.; Jakes, R.; Goedert, M. *Nature* **1997**, 388, 839.
- (11) Bussell, R., Jr.; Eliezer, D. *J. Mol. Biol.* **2003**, 329, 763.
- (12) Bartels, T.; Ahlstrom, L. S.; Leftin, A.; Kamp, F.; Haass, C.; Brown, M. F.; Beyer, K. *Biophys. J.* **2010**, 99, 2116.
- (13) Vamvaca, K.; Volles, M. J.; Lansbury, P. T., Jr. *J. Mol. Biol.* **2009**, 389, 413.
- (14) Meuvissen, J.; Gerard, M.; Desender, L.; Baekelandt, V.; Engelborghs, Y. *Biochemistry* **2010**, 49, 9345.
- (15) Wu, K. P.; Weinstock, D. S.; Narayanan, C.; Levy, R. M.; Baum, J. *J. Mol. Biol.* **2009**, 391, 784.
- (16) Hoyer, W.; Antony, T.; Cherny, D.; Heim, G.; Jovin, T. M.; Subramaniam, V. *J. Mol. Biol.* **2002**, 322, 383.
- (17) Hong, D. P.; Xiong, W.; Chang, J. Y.; Jiang, C. *FEBS Lett.* **2011**, 585, 561.
- (18) Fernandez, C. O.; Hoyer, W.; Zweckstetter, M.; Jares-Erijman, E. A.; Subramaniam, V.; Griesinger, C.; Jovin, T. M. *EMBO J.* **2004**, 23, 2039.
- (19) Wu, K.-P.; Baum, J. *J. Am. Chem. Soc.* **2010**, 132, 5546.
- (20) Wu, K. P.; Kim, S.; Fela, D. A.; Baum, J. *J. Mol. Biol.* **2008**, 378, 1104.
- (21) Dedmon, M. M.; Lindorff-Larsen, K.; Christodoulou, J.; Vendruscolo, M.; Dobson, C. M. *J. Am. Chem. Soc.* **2004**, 127, 476.
- (22) Bartels, T.; Choi, J. G.; Selkoe, D. J. *Nature* **2011**, 477, 107.
- (23) Jao, C. C.; Hegde, B. G.; Chen, J.; Haworth, I. S.; Langen, R. *Proc. Natl. Acad. Sci. U.S.A.* **2008**, 105, 19666.
- (24) Jao, C. C.; Der-Sarkissian, A.; Chen, J.; Langen, R. *Proc. Natl. Acad. Sci. U.S.A.* **2004**, 101, 8331.
- (25) Drescher, M.; Rooijen, B. D. v.; Veldhuis, G.; Subramaniam, V.; Huber, M. *J. Am. Chem. Soc.* **2010**, 132, 4080.
- (26) Middleton, E. R.; Rhoades, E. *Biophys. J.* **2010**, 99, 2279.
- (27) Zhu, M.; Li, J.; Fink, A. L. *J. Biol. Chem.* **2003**, 278, 40186.
- (28) Ferreon, A. C.; Gambin, Y.; Lemke, E. A.; Deniz, A. A. *Proc. Natl. Acad. Sci. U.S.A.* **2009**, 106, 5645.
- (29) Ferreon, A. C. M.; Deniz, A. A. *Biochemistry* **2007**, 46, 4499.
- (30) Ulmer, T. S.; Bax, A.; Cole, N. B.; Nussbaum, R. L. *J. Biol. Chem.* **2005**, 280, 9595.
- (31) Ferreon, A. C.; Moran, C. R.; Ferreon, J. C.; Deniz, A. A. *Angew. Chem.* **2010**, 49, 3469.
- (32) Giehm, L.; Oliveira, C. L.; Christiansen, G.; Pedersen, J. S.; Otzen, D. E. *J. Mol. Biol.* **2010**, 401, 115.
- (33) Bisaglia, M.; Tessari, I.; Pinato, L.; Bellanda, M.; Giraldo, S.; Fasano, M.; Bergantino, E.; Bubacco, L.; Mammi, S. *Biochemistry* **2004**, 44, 329.
- (34) Gambin, Y.; VanDelinder, V.; Ferreon, A. C. M.; Lemke, E. A.; Groisman, A.; Deniz, A. A. *Nat. Meth.* **2011**, 8, 239.

- (35) Bortolus, M.; Tombolato, F.; Tessari, I.; Bisaglia, M.; Mammi, S.; Bubacco, L.; Ferrarini, A.; Maniero, A. L. *J. Am. Chem. Soc.* **2008**, *130*, 6690.
- (36) Li, C.; Lutz, E. A.; Slade, K. M.; Ruf, R. A. S.; Wang, G.-F.; Pielak, G. J. *Biochemistry* **2009**, *48*, 8578.
- (37) Ahmad, M. F.; Ramakrishna, T.; Raman, B.; Rao Ch, , M. *J. Mol. Biol.* **2006**, *364*, 1061.
- (38) Mihajlovic, M.; Lazaridis, T. *Proteins: Struct. Funct. Bioinf.* **2008**, *70*, 761.
- (39) Perlmutter, J. D.; Braun, A. R.; Sachs, J. N. *J. Biol. Chem.* **2009**, *284*, 7177.
- (40) Shapiro, A. L.; Vinuela, E.; Maizel, J. V. *Biochem. Biophys. Res. Commun.* **1967**, *28*, 815.
- (41) Bhuyan, A. K. *Biopolymers* **2010**, *93*, 186.
- (42) Shaw, B. F.; Schneider, G. F.; Arthanari, H.; Narovlyansky, M.; Moustakas, D.; Durazo, A.; Wagner, G.; Whitesides, G. M. *J. Am. Chem. Soc.* **2011**.
- (43) Zhang, X. L.; Penfold, J.; Thomas, R. K.; Tucker, I. M.; Petkov, J. T.; Bent, J.; Cox, A.; Grillo, I. *Langmuir* **2011**, *27*, 10514.
- (44) Shiraham, K.; Tsujii, K.; Takagi, T. *J. Biochem.* **1974**, *75*, 309.
- (45) Georgieva, E. R.; Ramlall, T. F.; Borbat, P. P.; Freed, J. H.; Eliezer, D. *J. Biol. Chem.* **2010**, *285*, 28261.
- (46) Sammalkorpi, M.; Karttunen, M.; Haataja, M. *J. Phys. Chem. B* **2007**, *111*, 11722.
- (47) Sammalkorpi, M.; Karttunen, M.; Haataja, M. *J. Phys. Chem. B* **2009**, *113*, 5863.
- (48) Best, R. B.; Hummer, G. *J. Phys. Chem. B* **2009**, *113*, 9004.
- (49) Nguyen, P. H.; Li, M. S.; Derreumaux, P. *Phys. Chem. Chem. Phys.: PCCP* **2011**, *13*, 9778.
- (50) Hess, B.; Kutzner, C.; van der Spoel, D.; Lindahl, E. *J. Chem. Theory Comput.* **2008**, *4*, 435.
- (51) Sgourakis, N. G.; Yan, Y.; McCallum, S. A.; Wang, C.; Garcia, A. *E. J. Mol. Biol.* **2007**, *368*, 1448.
- (52) Hoover, W. G. *Phys. Rev. A* **1985**, *31*, 1695.
- (53) Nose, S. *Mal. Phys.* **1984**, *52*, 255.
- (54) Parrinello, M.; Rahman, A. *J. Appl. Phys.* **1981**, *52*, 7182.
- (55) Essmann, U.; Perera, L.; Berkowitz, M. L.; Darden, T.; Lee, H.; Pedersen, L. G. *J. Chem. Phys.* **1995**, *103*, 8577.
- (56) Miyamoto, S.; Kollman, P. A. *J. Comput. Chem.* **1992**, *13*, 952.
- (57) Hess, B.; Bekker, H.; Berendsen, H. J. C.; Fraaije, J. G. E. M. *J. Comput. Chem.* **1997**, *18*, 1463.
- (58) Wang, G.; Dale Treleaven, W.; Cushley, R. J. *Biochim. Biophys. Acta (BBA)—Lipids Lipid Metabolism* **1996**, *1301*, 174.
- (59) Humphrey, W.; Dalke, A.; Schulten, K. *J. Mol. Graphics* **1996**, *14*, 33.
- (60) Tian, J.; Garcia, A. E. *Biophys. J.* **2009**, *96*, L57.
- (61) Tian, J.; Garcia, A. E. *J. Chem. Phys.* **2011**, *134*.
- (62) Drescher, M.; Godschalk, F.; Veldhuis, G.; van Rooijen, B. D.; Subramaniam, V.; Huber, M. *ChemBioChem* **2008**, *9*, 2411.
- (63) Vilar, M.; Chou, H.-T.; Luehrs, T.; Maji, S. K.; Riek-Lohr, D.; Verel, R.; Manning, G.; Stahlberg, H.; Riek, R. *Proc. Natl. Acad. Sci. U.S.A.* **2008**, *105*, 8637.
- (64) Bodner, C. R.; Dobson, C. M.; Bax, A. *J. Mol. Biol.* **2009**, *390*, 775.
- (65) Bodner, C. R.; Maltsev, A. S.; Dobson, C. M.; Bax, A. *Biochemistry* **2010**, *49*, 862.